Calibration of Fe-57 isomer shift from ab initio calculations

Kurian, Reshmi; Filatov, Michael

Published in:
Physical Chemistry Chemical Physics

DOI:
10.1039/b918655g

Publication date:
2010

Calibration of ^{57}Fe isomer shift from *ab initio* calculations: can theory and experiment reach an agreement?

Reshmi Kurian and Michael Filatov*

Received 8th September 2009, Accepted 6th January 2010
First published as an Advance Article on the web 1st February 2010
DOI: 10.1039/b918655g

Using linear response approach to the Mössbauer isomer shift, the calibration constant $\alpha(^{57}\text{Fe})$ was obtained from high level *ab initio* calculations carried out for a representative set of iron compounds. The importance of the effects of relativity and electron correlation for an accurate description of the ^{57}Fe isomer shift is demonstrated on the basis of the Hartree–Fock, coupled cluster with singles and doubles and of the double hybrid density functional calculations. A reliable value of the calibration constant ($\alpha(^{57}\text{Fe}) = -0.306 \pm 0.009$ mm s^{-1}) was obtained with the use of the B2-PLYP double hybrid density functional. This value is in good agreement with the experimentally estimated constant of $-0.31 \pm 0.04\ a_0^3$ mm s^{-1} and can be recommended for theoretical modeling of ^{57}Fe isomer shifts.

I. Introduction

Since its discovery 50 years ago, Mössbauer spectroscopy has become a versatile tool of chemical analysis capable of providing information about the chemical environment of the resonating nucleus on an atomic scale.[1–4] The most well-known application of Mössbauer spectroscopy is the determination of iron ^{57}Fe in crystalline and in disordered solid samples which finds an increasing number of applications in biochemistry and biophysics as well as in materials science, nano-science, and catalysis.[5–7] The parameters of Mössbauer spectra, such as the isomer shift, quadrupole splitting, magnetic hyperfine splitting, are sensitive characteristics of the electronic structure and depend on the electron density distribution in the vicinity of the resonating nucleus. Thus, the isomer shift of the Mössbauer spectrum is commonly related to the so-called contact density,[8–11]

$$\delta = \alpha(\bar{\rho}^{(a)} - \bar{\rho}^{(s)}) \quad (1)$$

where the calibration constant α depends on the parameters of the nuclear γ-transition. Because the isomer shift is a relative quantity, it is expressed in eqn (1) *via* a difference between the contact density in the target compound $\bar{\rho}^{(a)}$ and in the reference compound $\bar{\rho}^{(s)}$. Usually, the parameters of the nuclear γ-transition, such as the variation of the nuclear charge radius, are not known experimentally with sufficiently high accuracy, such that a direct determination of α is not possible.

Usually, the calibration constant is evaluated from a comparison of the theoretically estimated contact densities with the experimentally observed isomer shifts.[8–13] In this calibration procedure, a linear regression equation is used,

$$\delta = \alpha\bar{\rho} - b \quad (2)$$

where the parameters α and b are determined from the least squares fit. Although a very good linear correlation between δ and $\bar{\rho}$ was obtained in many works, the value of α varied in a wide range depending on the method of calculation and a set of experimental isomer shifts employed in the calibration. Thus, for iron ^{57}Fe a "consensus" value of $-0.267 \pm 0.115\ a_0^3$ mm s^{-1} was suggested by Oldfield from a compilation of the published $\alpha(^{57}\text{Fe})$ constants.[14] Wide error bars in this value imply that there is no clear convergence of the estimated calibration constants to a single value.

Besides theoretical calculations, the contact densities can be evaluated from the experimentally measured life times of electron capture by atomic nuclei. Thus, a value of $-0.31 \pm 0.04\ a_0^3$ mm s^{-1} was derived by Ladrière *et al.*[15] from the life-time measurements of electron capture by the ^{52}Fe nucleus. Because the electron capture rate is proportional to the contact density $\bar{\rho}$, the $\alpha(^{57}\text{Fe})$ calibration constant could be obtained from a comparison of the measured life times with the ^{57}Fe isomer shifts in the same compounds.

A substantial difference between this value and a theoretically estimated "consensus" value of $\alpha(^{57}\text{Fe})$ suggests that certain shortcomings of theoretical calculations need to be improved. In particular, the effects of relativity and electron correlation, which strongly modify the electron distribution in the vicinity of the nucleus, need to be accurately taken into account. This can be achieved with the use of the linear response theory, in which the isomer shift is treated as a derivative of the total electronic energy E_e with respect to the charge radius R of the resonating nucleus.[16] For convenience, the isomer shift is expressed *via* eqn (1) where the contact densities are obtained from[16]

$$\bar{\rho} = \frac{5}{4\pi ZR}\frac{\delta E_e(R)}{\delta R}\bigg|_{R=R_0} \quad (3)$$

in which R_0 is the experimental value of the nuclear charge radius for the given isotope (*e.g.* ^{57}Fe). Note that this formalism requires the use of finite size nucleus model in the

Theoretical Chemistry, Zernike Institute for Advanced Materials, Rijksuniversiteit Groningen, Nijenborgh 4, 9747 AG Groningen, The Netherlands. E-mail: m.filatov@rug.nl

calculations. Previously this formalism was applied to the calibration of the isomer shift of ^{119}Sn which demonstrated high reliability of the method.[17]

In the present work, we apply the linear response formalism[16] to the calibration of ^{57}Fe isomer shift on the basis of *ab initio* calculations carried out with the wave function theory methods, such as the Hartree–Fock method, the second-order Møller–Plesset (MP2) perturbation theory method, the coupled-cluster method, as well as with a density functional method B2-PLYP, the double hybrid density functional developed recently by Grimme.[18] The major purpose of this work is to apply the most accurate computational schemes in combination with large un-contracted basis sets to obtain a reliable value of the $\alpha(^{57}\mathrm{Fe})$ calibration constant. A representative number of iron-containing solid compounds (crystalline solids and matrix isolated molecules) is employed in the calibration with the use of the embedded cluster approach. In a series of atomic calculations, for various oxidation states of iron atom, the importance of the proper account of relativity and electron correlation is demonstrated.

II. Details of calculations

The calculations are carried out in the embedded cluster approach, where a cluster of atoms representing the structural unit of the crystalline solid is immersed in the Madelung field of the rest of the crystal. The Madelung field is modeled by the field of a large array of point charges placed at the appropriate crystallographic positions. The magnitudes of the charges are determined from the natural bond order (NBO) analysis[19] of the respective cluster wave functions calculated at the Hartee–Fock level.

The iron compounds used in this work are FeF_2, $KFeF_3$, $[Fe(H_2O)_6]^{2+}$, $FeBr_2$, $FeCl_2$, FeI_2, $[Fe(H_2O)_6]^{3+}$, FeF_3, $FeCp_2$, $K_4Fe(CN)_6$, $K_3Fe(CN)_6$, $Fe(CO)_5$, K_2FeO_4. The clusters representing these compounds are reported in Table 1 along with the respective literature references. In the embedded cluster calculations, the cations nearest to the cluster were represented with the use of the respective Stuttgart effective core potentials (ECPs).[20] For matrix isolated compounds, the polarizable continuum model (PCM)[21] was employed to model environment's effects.

The calculations are carried out using the COLOGNE 2005[32] suite of programs in which the computational scheme for the isomer shift calculation is implemented. The relativistic effects are included using the normalized elimination of the small component (NESC) method[33] within the one-electron approximation.[34] The electron contact densities near the nucleus are calculated according to eqn (3). The derivatives $\frac{\delta E_e(R)}{\delta R}$ in eqn (3) are calculated numerically using the increment of 10^{-6} Bohr for the root mean square (r.m.s.) nuclear charge radius ($R_{Fe} = 0.70213 \times 10^{-4}$ Bohr). The calibration constant α is obtained from eqn (2) by linear regression of the calculated densities against the experimental isomer shifts. Throughout this work, the Gaussian nucleus model is used in the calculations.

The calculations are carried out using Hartree–Fock (HF), second order Møller–Plesset perturbation theory (MP2), coupled cluster singles and doubles with perturbative treatment of triple excitations (CCSD(T)) and double hybrid density functional (B2-PLYP) level. The 24s12p9d basis set of Partridge[35] with a set of polarization functions taken from TZVpp basis set of Ahlrichs and May[36] is used for iron and the correlation consistent double-zeta (cc-pVDZ) basis set of Dunning[37] is used for the neighboring atoms. All basis sets are used in the un-contracted form. The closed shell systems are treated with spin restricted formalism and the open-shell systems with spin unrestricted formalism.

Table 1 ^{57}Fe electron contact densities (a_0^{-3}) according to eqn (3) calculated with the use of relativistically corrected HF, MP2 and B2-PLYP methods. Literature references to crystal structures and representative clusters are given for each compound

Compound	Cluster	Reference	SCF[a]	MP2[a]	B2-PLYP[b]
1 FeF_2	$[FeF_6]^{4-}$	22	86.33	86.00	8.59
2 $KFeF_3$	$[FeF_6]^{4-}$	23	86.41	86.03	8.72
3 $[Fe(H_2O)_6]^{2+}$	$[Fe(H_2O)_6]^{2+}$	13	86.56	86.05	8.68
4 $FeBr_2$	$[FeBr_6]^{4-}$	22	87.31	87.16	9.74
5 $FeCl_2$	$[FeCl_6]^{4-}$	22	87.24	87.06	9.52
6 FeI_2	$[FeI_6]^{4-}$	24	88.03	88.14	10.51
7 $[Fe(H_2O)_6]^{3+}$	$[Fe(H_2O)_6]^{3+}$	13	90.35	89.92	11.75
8 FeF_3	$[FeF_6]^{3-}$	25	89.98	89.30	11.76
9 $FeCp_2$	$Fe(C_5H_5)_2$	26, 27	90.12	89.91	11.50
10 $K_4Fe(CN)_6$	$[Fe(CN)_6]^{4-}$	28	91.69	92.07	13.55
11 $K_3Fe(CN)_6$	$[Fe(CN)_6]^{3-}$	29	92.79	91.49	13.72
12 $Fe(CO)_5$	$Fe(CO)_5$	30	92.39	92.19	13.98
13 K_2FeO_4	$[FeO_4]^{2-}$	31	93.78	93.15	15.47

[a] A large constant of 14 800 a_0^{-3} has been subtracted from all the values. [b] A large constant of 15 000 a_0^{-3} has been subtracted from all the values.

III. Results and discussion

In this section we apply the linear response approach[16] to the calibration of ^{57}Fe Mössbauer isomer shift in a series of compounds described in the previous section. Before we start with the calculations on cluster models, we would like to demonstrate the importance of inclusion of the effects of relativity and electron correlation into the calculation of the isomer shift.

Traditionally, for elements as light as ^{57}Fe, an approach based on the use of the contact densities obtained from the non-relativistic calculations with the point-like nucleus is employed.[9–11] Because relativity strongly modifies the wave function and the electron density in the vicinity of the nucleus, the use of the non-relativistic contact density $\bar{\rho} = \rho(0)$ (where $\rho(0)$ denotes the electron density at the nuclear position) may lead to considerable errors even for a light element. This is illustrated in Fig. 1, where the contact density differences $\Delta\bar{\rho}(Fe^{n+}) = \bar{\rho}(Fe^{n+}) - \bar{\rho}(Fe^0)$ calculated within the linear response formalism[16] for a series of iron ions are shown. In this Figure, the contact density differences obtained from the relativistically corrected CCSD(T) atomic calculations are compared with those obtained in the non-relativistic CCSD(T) calculations for the ground states of respective iron ions. When taking the density differences, the non-relativistic contact densities are scaled with a factor $\rho_{rel}(Fe^0)/\rho_{nr}(Fe^0)$ which agrees with the commonly adopted prescription of scaling of the non-relativistic contact densities.[8–14] It can be seen that relativity has a noticeable effect on the density differences and, in some cases (*e.g.*, Fe^+ and Fe^{4+}), may

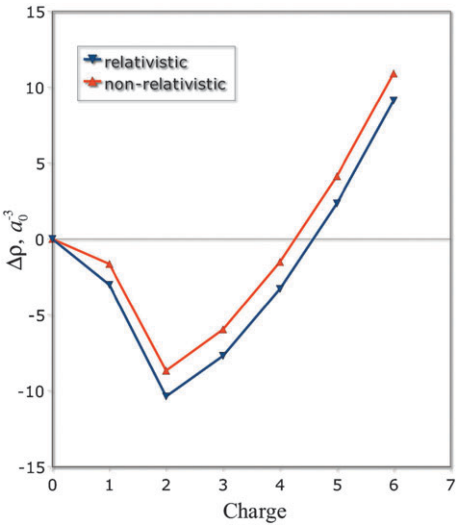

Fig. 1 Contact density difference $\Delta\bar{\rho}(Fe^{n+}) = \bar{\rho}(Fe^{n+}) - \bar{\rho}(Fe^{0})$ as a function of metal charge n. All calculations are carried out for the isolated Fe^{n+} atoms in the respective high-spin ground states with the use of the non-relativistic and relativistically corrected CCSD(T) method (see the legend).

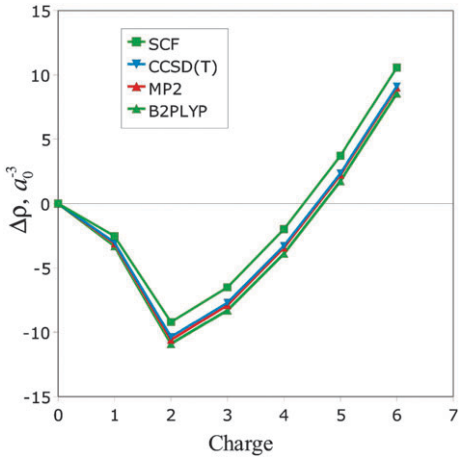

Fig. 2 Contact density difference $\Delta\bar{\rho}(Fe^{n+}) = \bar{\rho}(Fe^{n+}) - \bar{\rho}(Fe^{0})$ as a function of metal charge n. All calculations are carried out for the isolated Fe^{n+} atoms in the respective high-spin ground states with the use of the relativistically corrected HF, CCSD(T), MP2, and B2-PLYP methods (see the legend).

account for up to 50% of the total density variation. Furthermore, scaling of the non-relativistic density does not provide a sufficiently accurate account of relativistic effects on the difference densities. Because the isomer shift is a relative quantity and depends on the density differences rather than on the total contact densities, the importance of the proper account of relativity is obvious from Fig. 1.

Another factor which can modify the density distribution is the electron correlation. The importance of electron correlation for the contact densities is illustrated in Fig. 2, where the density differences $\Delta\bar{\rho}(Fe^{n+}) = \bar{\rho}(Fe^{n+}) - \bar{\rho}(Fe^{0})$ obtained in the relativistically corrected Hartree–Fock, CCSD(T), and B2-PLYP calculations for a series of iron ions are shown. From comparison of the HF and CCSD(T) density differences, it is obvious that electron correlation makes a noticeable contribution to the overall density variation, especially for highly charged ions. It is noteworthy that the results of the B2-PLYP calculations closely match the CCSD(T) results. This observation suggests that the B2-PLYP density functional can be used in the calculations on cluster models of solids instead of the CCSD(T) method, which should lead to a considerable saving of computation time. A similar conclusion on the high accuracy of the B2-PLYP functional in the isomer shift calculations has been recently made by Römelt, Ye and Neese.[12]

Table 1 reports the contact densities (eqn (3)) calculated with the use of the relativistically corrected HF, MP2, and B2-PLYP methods. These densities are used in the linear regression analysis with eqn (2) the results of which are plotted in Fig. 3. The parameters of linear fit (eqn (2)) are used to calculate the isomer shifts which are reported in Table 2. The values of the calibration constant obtained with different methods, $\alpha_{HF}(^{57}Fe) = -0.265 \pm 0.009\ a_0^3$ mm s^{-1}, $\alpha_{MP2}(^{57}Fe) = -0.271 \pm 0.013\ a_0^3$ mm s^{-1}, and $\alpha_{B2\text{-}PLYP}(^{57}Fe) = -0.306 \pm 0.009\ a_0^3$ mm s^{-1}, approach the experimental estimate of $-0.31 \pm 0.04\ a_0^3$ mm s^{-1} [15] with increasing accuracy of the electron correlation description in the sequence HF < MP2 < B2-PLYP.

The B2-PLYP calculations provide the most reliable value of the calibration constant $\alpha_{B2\text{-}PLYP}(^{57}Fe) = -0.306 \pm 0.009\ a_0^3$ mm s^{-1} as evidenced by the smallest mean absolute deviation ($0.047\ a_0^3$ mm s^{-1}) and the standard deviation ($0.072\ a_0^3$ mm s^{-1}) of the calculated isomer shifts from the experimental values presented in Table 2. To test the reliability of the obtained calibration constants we have undertaken calculations of the relative isomer shifts $\Delta\delta^x = \delta^x - \delta^{ref}$ by choosing different reference compounds. The results of these calculations are collected in lower part of Table 2, where the relative shifts $\Delta\delta^x$ calculated with respect to $K_4Fe(CN)_6$, $KFeF_3$, FeF_3, and K_2FeO_4 are shown. It is seen that the use of the B2-PLYP method and the $\alpha_{B2\text{-}PLYP}(^{57}Fe)$ calibration constant leads to the best correlation with the experimental values of the relative shifts irrespective of the reference compound selected. Thus we can conclude that the $\alpha_{B2\text{-}PLYP}(^{57}Fe)$ value of $-0.306 \pm 0.009\ a_0^3$ mm s^{-1} is the most reliable theoretical value of the calibration constant obtained in this work. It is gratifying that this value is in a very good agreement with the experimental estimate of $-0.31 \pm 0.04\ a_0^3$ mm s^{-1} for the ^{57}Fe calibration constant.[15] Note that the $\alpha_{B2\text{-}PLYP}$ constant obtained in this work is in a good agreement with the value $-0.311\ a_0^3$ mm s^{-1} obtained by Römelt, Ye and Neese from the B2-PLYP calculations employing the quasi-relativistic ZORA Hamiltonian,[12] however it is somewhat lower in the absolute value than the constant $-0.336\ a_0^3$ mm s^{-1} obtained in the non-relativistic B2-PLYP calculations.[12]

IV. Conclusions

In this work, we have undertaken calibration of the ^{57}Fe isomer shift using the relativistically corrected high level *ab initio* calculations. With the use of linear response approach to the isomer shift[16] the importance of proper description of the effects of relativity and electron correlation for the theoretical

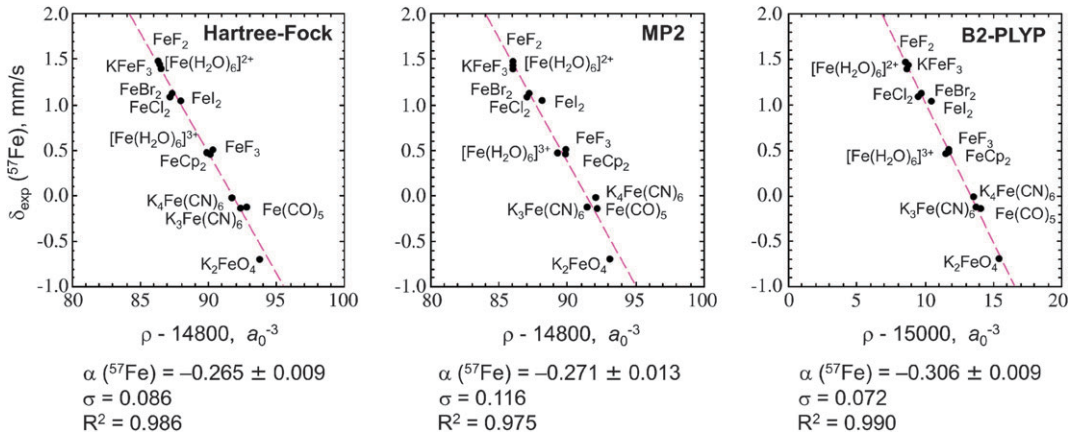

Fig. 3 Linear regression of the contact densities calculated with the relativistically corrected HF, MP2 and B2-PLYP methods for a series of iron compounds against the experimental isomer shifts. Calibration constant α (in a_0^3 mm s^{-1}), Pearson's correlation coefficient R^2 and standard deviation σ (in mm s^{-1}) are given for each method.

Table 2 ^{57}Fe isomer shifts (in mm s^{-1}) obtained from a linear regression, eqn (2), of the densities reported in Table 1 against the experimental shifts. For each computational method, the parameters of eqn (2) as well as Pearson's correlation coefficient R^2 and standard deviation σ are given. Mean absolute error and standard deviation in the relative isomer shifts $\Delta\delta^x = \delta^x - \delta^{ref}$ (in mm s^{-1}) calculated with respect to different compounds are given in the lower part of the table

	δ_{exp}	SCF	MP2	B2-PLYP
1 FeF_2	1.467	1.445	1.461	1.460
2 $KFeF_3$	1.440	1.424	1.453	1.420
3 $[Fe(H_2O)_6]^{2+}$	1.390	1.384	1.447	1.432
4 $FeBr_2$	1.120	1.185	1.146	1.108
5 $FeCl_2$	1.092	1.204	1.173	1.175
6 FeI_2	1.044	0.995	0.880	0.872
7 $[Fe(H_2O)_6]^{3+}$	0.500	0.381	0.398	0.493
8 FeF_3	0.480	0.479	0.566	0.489
9 $FeCp_2$	0.460	0.442	0.400	0.569
10 $K_4Fe(CN)_6$	−0.020	0.026	−0.186	−0.058
11 $K_3Fe(CN)_6$	−0.130	−0.265	−0.028	−0.110
12 $Fe(CO)_5$	−0.140	−0.159	−0.218	−0.190
13 K_2FeO_4	−0.690	−0.527	−0.478	−0.646
α/a_0^3 mm s^{-1}		−0.265 ± 0.009	−0.271 ± 0.013	−0.306 ± 0.009
b/mm s^{-1}		3941.6 ± 140.2	4038.6 ± 194.0	4595.4 ± 136.3
R^2		0.986	0.975	0.990
M.A.E./mm s^{-1} [a]		0.059	0.089	0.047
σ/mm s^{-1} [b]		0.086	0.116	0.072
With respect to $K_4Fe(CN)_6$				
M.A.E./mm s^{-1}		0.0836	0.1793	0.0658
σ/mm s^{-1}		0.0998	0.2140	0.0833
With respect to $KFeF_3$				
M.A.E./mm s^{-1}		0.0618	0.0949	0.0551
σ/mm s^{-1}		0.0881	0.1166	0.0753
With respect to FeF_3				
M.A.E./mm s^{-1}		0.0639	0.1165	0.0523
σ/mm s^{-1}		0.0863	0.1486	0.0729
With respect to K_2FeO_4				
M.A.E./mm s^{-1}		0.1765	0.2292	0.0649
σ/mm s^{-1}		0.1970	0.2575	0.0865

[a] Mean absolute error. [b] Standard deviation.

contact densities was demonstrated. In the calculations for a series of iron ions, it was shown that relativity and electron correlation may account for up to *ca.* 50% of the contact density differences which are important for the isomer shift.

With the use of relativistically corrected HF, MP2, and B2-PLYP methods the values of the calibration constant $\alpha(^{57}Fe)$ were obtained from a linear regression of the contact densities calculated for a large number of iron compounds modeled within the embedded cluster approach against the experimental isomer shift values. The most reliable theoretical value of -0.306 ± 0.009 a_0^3 mm s^{-1} was obtained with the use of the B2-PLYP method which provides the best statistical correlation ($R^2 = 0.990$ and $\sigma = 0.072$ a_0^3 mm s^{-1}) with the experimental data. The reliability of the obtained calibration constant was also verified in the calculation of the relative isomer shifts $\Delta\delta^x = \delta^x - \delta^{ref}$ using different iron compounds

as a reference. In all cases, the B2-PLYP method with $\alpha_{\text{B2-PLYP}}(^{57}\text{Fe}) = -0.306 \pm 0.009\ a_0^3\ \text{mm s}^{-1}$ yielded the least deviations from the experimental data. It is noteworthy that this theoretical value is in a very good agreement with the experimental estimate of $-0.31 \pm 0.04\ a_0^3$ mm s^{-1}.[15] This observation suggests that the $\alpha(^{57}\text{Fe})$ value obtained in this work can be used as a universal constant in theoretical modeling of the Mössbauer isomer shift.

References

1 O. Leupold, J. Pollmann, E. Gerdau, H. D. Rüter, G. Faigel, M. Tegze, G. Bortel, R. Rüffer, A. I. Chumakov and A. Q. R. Baron, *Europhys. Lett*., 1996, **35**, 671–6.
2 I. Koyama, Y. Yoda, X. W. Zhang, M. Ando and S. Kikuta, *Jpn. J. Appl. Phys*., 1996, **35**, 6297–300; G. Neyens, J. Odeurs, R. Coussement, C. L'abbé, S. Cottenier and J. Ladriére, *Hyperfine Interact*., 1998, **111**, 341–4; O. Leupold, A. I. Chumakov, E. E. Alp, W. Sturhahn and A. Q. R. Baron, *Hyperfine Interact*., 1999, **123–124**, 611–31; C. L'abbé, R. Callens and J. Odeurs, *Hyperfine Interact*., 2001, **135**, 275–94; D. A. Shirley and H. Haas, *Annu. Rev. Phys. Chem*., 1972, **23**, 385–414.
3 R. Coussement, S. Cottenier and C. L'abbé, *Phys. Rev. B: Condens. Matter*, 1996, **54**, 16003–9.
4 A. Konjhodzic, A. Adamczyk, F. Vagizov, Z. Hasan, E. E. Alp, W. Sturhahn, Jiyong Zhao and J. J. Carroll, *Hyperfine Interact*., 2006, **170**, 83–9.
5 E. Münck, in *Physical Methods in Bioinorganic Chemistry: Spectroscopy and Magnetism*, ed. L. Que, Jr., University Science Books, Sausalito, 2000, p. 287; E. Münck and A. Stubna, in *Comprehensive Coordination Chemistry II*, ed. A. B. P. Lever, Elsevier, NewYork, 2002, vol. 2, p. 279.
6 S. Mørup, *Mössbauer Effect Ref. Data J*., 2002, **25**, 105.
7 Yu. M. Kagan and I. S. Lyubutin, in *Applications of the Mössbauer Effect*, Gordon and Breach, New York, 1985, vol. 4.
8 W. C. Nieuwpoort, D. Post and P. T. van Duijnen, *Phys. Rev. B: Condens. Matter*, 1978, **17**, 91–8.
9 G. K. Wertheim, in *Mossbauer Effect: Principles and Applications*, Academic Press, New York, 1964; G. K. Shenoy and B. D. Dunlap in *Mössbauer Isomer Shifts*, ed. G. K. Shenoy and F. E. Wagner, North-Holland, Amsterdam, 1978, pp. 869–94; L. R. Walker, G. K. Wertheim and V. Jaccarino, *Phys. Rev. Lett*., 1961, **6**, 98–101.
10 D. A. Shirley, *Rev. Mod. Phys*., 1964, **36**, 339–51.
11 P. Gütlich, R. Link and A. Trautwein, in *Mössbauer Spectroscopy and Transition Metal Chemistry*, Springer, Heidelberg, 1978.
12 M. Römelt, S. Ye and F. Neese, *Inorg. Chem*., 2009, **48**, 784–5; F. Neese, *Inorg. Chim. Acta*, 2002, **337**, 181–92; S. Sinnecker, L. D. Slep, E. Bill and F. Neese, *Inorg. Chem*., 2005, **44**, 2245–54.
13 A. Sadoc, R. Broer and C. de Graaf, *Chem. Phys. Lett*., 2008, **454**, 196–200.
14 Y. Zhang, J. Mao and E. Oldfield, *J. Am. Chem. Soc*., 2002, **124**, 7829–39.
15 J. Ladrière, A. Meykens, R. Coussement, M. Cogneau, M. Boge, P. Auric, R. Bouchez, A. Benabed and J. Godard, *J. Phys., Coll. C2*, 1979, **40**, 20.
16 M. Filatov, *J. Chem. Phys*., 2007, **127**, 084101.
17 R. Kurian and M. Filatov, *J. Chem. Phys*., 2009, **130**, 124121.
18 S. Grimme, *J. Chem. Phys*., 2006, **124**, 034108.
19 J. E. Carpenter and F. Weinhold, *THEOCHEM*, 1988, **169**, 41; J. P. Foster and F. Weinhold, *J. Am. Chem. Soc*., 1980, **102**, 7211–8; A. E. Reed and F. Weinhold, *J. Chem. Phys*., 1983, **78**, 4066; A. E. Reed, R. B. Weinstock and F. Weinhold, *J. Chem. Phys*., 1985, **83**, 735.
20 P. Fuentealba, L. von Szentpaly, H. Preuss and H. Stoll, *J. Phys. B: At. Mol. Phys*., 1985, **18**, 1287–96.
21 J. Tomasi, B. Mennucci and R. Cammi, *Chem. Rev*., 2005, **105**, 2999.
22 U. D. Wdowik and K. Ruebenbauer, *Phys. Rev. B: Condens. Matter Mater. Phys*., 2007, **76**, 155118.
23 K. Knox, *Acta Crystallogr*., 1961, **14**, 583–5.
24 J. Gerald, A. R. Fert, P. Meriel and Y. Allain, *Solid State Commun*., 1974, **14**, 187.
25 M. A. Hepworth, R. H. Jack, R. D. Peacock and G. J. Westland, *Acta Crystallogr*., 1957, **10**, 63–9.
26 A. Haaland, *Top. Curr. Chem*., 1975, **53**, 1.
27 J. D. Dunitz, L. E. Orgel and A. Rich, *Acta Crystallogr*., 1956, **9**, 373–5.
28 R. Kiriyama, H. Kiriyama and T. Wada, *J. Phys. Soc. Jpn*., 1964, **19**, 540–9.
29 B. N. Figgis, M. Gerloch and R. Mason, *Proc. R. Soc. London, Ser. A*, 1969, **309**, 91–118.
30 W. Kerler, W. Neuwirth and E. Fluck, *Z. Phys*., 1963, **175**, 200.
31 M. L. Hoppe, E. O. Schlemper and R. K. Murmann, *Acta Crystallogr., Sect. B: Struct. Crystallogr. Cryst. Chem*., 1982, **38**, 2237–9.
32 E. Kraka, J. Gräfenstein, M. Filatov, V. Polo, A. Wu, Y. He, L. Olsson, Z. Konkoli, Z. He, J. Gauss, F. Reichel and D. Cremer, in *COLOGNE 2005*, Göteborg University, Göteborg, 2005.
33 K. G. Dyall, *J. Chem. Phys*., 1997, **106**, 9618–26; M. Filatov and K. G. Dyall, *Theor. Chem. Acc*., 2007, **117**, 333–8.
34 K. G. Dyall, *J. Chem. Phys*., 2001, **115**, 9136; K. G. Dyall, *J. Comput. Chem*., 2002, **23**, 786–93.
35 H. Patridge, *J. Chem. Phys*., 1987, **87**, 6643–7.
36 R. Ahlrichs and K. May, *Phys. Chem. Chem. Phys*., 2000, **2**, 943–5.
37 T. H. Dunning, Jr., *J. Chem. Phys*., 1989, **90**, 1007–23.

